Charge-Exchange Collisions Between Helium Ions and Cesium Vapor in the Energy Range 1.5–25 keV

A. S. Schlachter, D. H. Loyd, P. J. Bjorkholm, L. W. Anderson, and W. Haeberli
University of Wisconsin, Madison, Wisconsin
(Received 13 May 1968)

Charge-exchange collisions have been studied when He^+ ions with an energy in the range 1.5–25 keV are incident on Cs vapor. Measurements of the positive, neutral, and negative beam components after passage through the target were made as a function of the Cs target density at twelve energies. Over the entire energy range studied, the negative fraction was found to reach a maximum and then decrease with increasing target density. The maximum yield of He^- ions was measured to be $(1.4 \pm 0.1)\%$. The maximum occurred at a He^+ energy of 6 keV and a Cs target thickness of 5×10^{14} atoms/cm^2. Various cross sections relevant to the charge-exchange process were determined. At 10 keV the cross section for the production of a fast He^0 atom from a He^+ ion incident on Cs is $(6.3 \pm 0.6) \times 10^{-15}$ cm^2, the value of the cross section for the production of a He^0 atom when a He^- ion is incident on Cs is $(1.0 \pm 0.3) \times 10^{-14}$ cm^2, and the value for the production of a He^- ion when a fast He^0 atom in the (1s) (2s) $^3S_1$ state is incident on Cs is $(1.4 \pm 0.4) \times 10^{-16}$ cm^2.

I. INTRODUCTION

Charge-exchange collisions of He^+ ions on Cs vapor are of considerable interest because of the large yield of He^- ions and because of the general interest in studying electron-transfer cross sections. In the present experiment, a momentum-analyzed, collimated beam of 1.5–25-keV He^+ ions was passed through a Cs vapor target of variable thickness. The beam emerging from the target was separated into its various charge components by a magnetic field, and the positive, negative, and neutral components were measured simultaneously.

The customary notation for cross sections is used in this paper. The two subscripts refer to the initial and final states, respectively, of the He atom or ion. The subscripts $+$, $-$, t, and s refer, respectively, to He^+ ions, He^- ions [1], He^0 atoms in triplet states, and He^0 atoms in singlet states (as discussed in Sec. IV). The subscript 0 refers to all He^0 atoms irrespective of the state.

The following cross sections were determined: σ_{+0}, σ_{0-}, σ_{-0}, and σ_{t+}. Also determined, but with less precision, were σ_{t-}, σ_{s-}, σ_{+t}, σ_{+s}, and σ_{ts}. Upper bounds were determined for σ_{+-}, σ_{-+}, and σ_{st}. The only previous measurements of cross sections reported for He^+ incident on a Cs target are by Lorents and Peterson, [2] who measured σ_{+0} at energies up to 1.5 keV by a crossed beam technique, and by Donnally and Thoeming, [3] who measured σ_{+0}, σ_{-0}, $(\sigma_{ts} + \sigma_{t-})$, and a lower bound on σ_{t-}, at 2 keV).

The maximum yield of He^- ions found in the present experiment is $(1.4 \pm 0.1\%)$, at a He^+ energy of 6 keV. This yield is very high relative to the yield in permanent gases, which is typically 0.02%. [4] The yield of He^- ions after charge exchange in Cs has previously been measured only in the range 1–3 keV by Donnally and Thoeming. [3] The He^- yields obtained by charge exchange in K have been reported as high as 1.7% by Ennis *et al.* [5] at an energy of 7 keV. Formation of He^0 metastable atoms by charge exchange in K has also been reported. [6] The high yield of He^- ions makes Cs or K useful as the charge-exchange medium in negative ion sources for a tandem electrostatic accelerator. Both Cs and K have been used for this purpose. [7-9]

II. APPARATUS AND MEASUREMENTS

The apparatus, shown in Fig. 1, consists of an ion source and associated equipment, a beam collimator, a charge-exchange target, and beam-measuring equipment.

He^+ ions are produced by a radio-frequency source, and are accelerated by a voltage which can

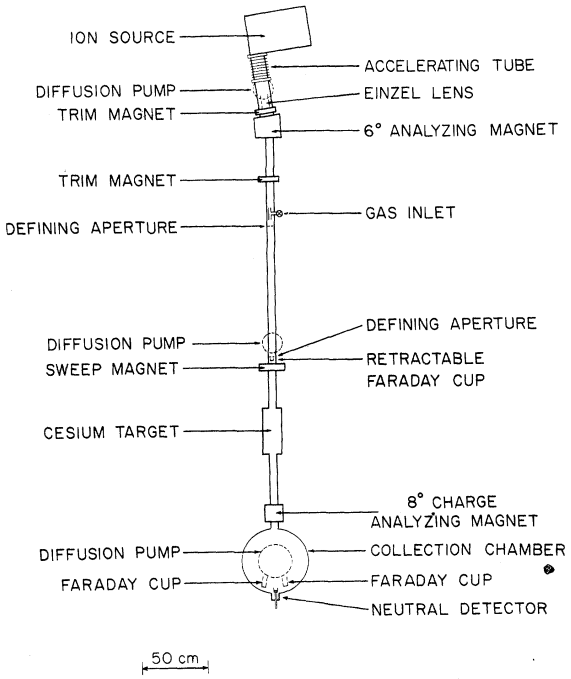

FIG. 1. Schematic diagram of apparatus. The gas inlet is not used in this experiment.

be varied from 1.5–25 keV. The ions pass through a unipotential lens (einzel lens), a six-degree analyzing magnet, and two vertical trim magnets. No further steering magnets are used. The accelerating voltage is measured to ±3%, using a wire-wound voltage divider and high-impedance voltmeter.

The beam is collimated by two 0.15-cm-diam apertures separated by a drift tube 1 m long. In front of each aperture are four insulated slits to monitor the current and to keep the beam centered on the aperture. The pressure in the drift tube is kept below 1×10^{-6} Torr to reduce charge exchange in the residual gas. The collimation section limits the beam to an angular divergence of 0.003 radians. This divergence is small enough to permit the beam to pass through the Cs oven and to enter the collection chamber without striking the entrance or exit apertures of the Cs oven, except when high Cs densities cause multiple scattering. Following the collimation section is a suppressed Faraday cup (hereafter called the source cup) to measure the positive beam incident on the Cs target. This cup can be retracted from the beam path to allow the beam to enter the charge-exchange target.

A horizontal coil which surrounds the entire apparatus is used to compensate for the vertical component of the earth's magnetic field. The horizontal component of the earth's field is nearly along the beam axis and hence does not affect the beam.

In front of the Cs oven is a coil producing a transverse magnetic field of sufficient strength to sweep charged particles out of the beam. This coil is used to determine the contribution to the measured beam currents by unwanted fast neutral atoms formed in the drift tube. This contribution is subtracted as background.

The Cs oven serving as the target for the charge-exchange collisions is shown in Fig. 2. The oven is a 10 cm-diam stainless-steel cylindrical container enclosing a tightly fitting copper liner, 20.8 cm long and 0.5 cm thick with copper end plates 1 cm thick. The beam entrance and exit tubes are 8.7-cm-long stainless-steel tubes with an inside diameter of 0.5 cm. The purpose of the stainless-steel end tubes is to reduce the gas conductance out of the oven for Cs. The oven is differentially pumped at each end by a diffusion pump and a liquid-nitrogen-cooled copper cylinder concentric with the beam axis. The copper oven is maintained typically at a temperature of 225°C. The end tubes are kept approximately 25° hotter to prevent Cs from condensing in the end tubes.

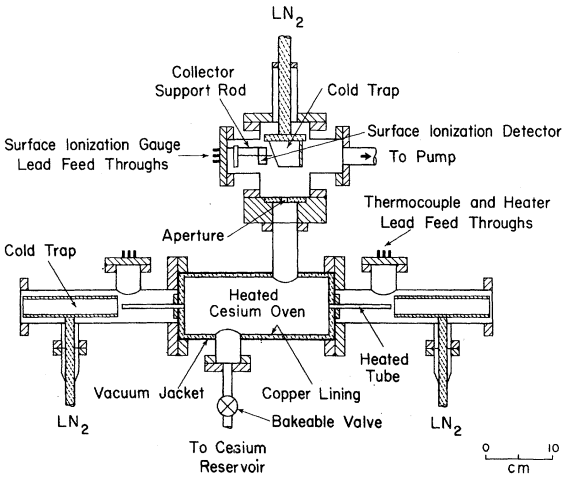

FIG. 2. Drawing of the Cs oven, which served as charge-exchange target, and of the Cs gauge, used to measure the density of Cs vapor in the Cs oven.

The effective path length for He ions in the Cs target is determined by consideration of the Cs density profile. The Cs vapor density is uniform inside the Cs oven, because the diameter of the oven is large relative to the diameter of all entrance and exit openings. The Cs density is nearly zero outside the heated end tubes which form the ion beam entrance and exit apertures of the Cs target, because of the very high pumping speed for Cs of the liquid-nitrogen-cooled traps located at the end of each tube (see Fig. 2). Since the end tubes are approximately 25° hotter than the Cs oven, no Cs condenses in these tubes and there is no source of Cs atoms in these tubes. Consequently, the Cs vapor density in each tube decreases linearly from the Cs oven density at one end to zero density at the other end as the Cs undergoes molecular flow from the Cs oven out each tube. The mean Cs density in each end tube is therefore half the density in the oven. The effective Cs path length is the length of the oven plus half the length of each end tube. This length is 30.5 cm.

The Cs is contained in a heated reservoir. The Cs vapor is admitted to the target chamber through a bakeable valve. The Cs density in the oven can be varied by changing the temperature of the reservoir or by operation of the valve between the reservoir and the oven. There is also provision for admitting argon into the oven for calibration measurements.

The gauge used to measure Cs density in the oven is a surface ionization detector.[10,12] This detector is located in an auxiliary heated stainless-steel chamber connected to the Cs oven by a 0.1-cm-diam aperture in a thin stainless-steel plate. Inside the chamber is a liquid-nitrogen-cooled copper trap with a surface area of approximately 150 cm^2. The pumping of Cs vapor by the cold surface and the low conductance of the inlet aperture combine to attenuate the Cs density in the auxiliary chamber relative to the Cs density in the target. The attenuation of the Cs density is necessary so that (1) space charge does not limit the Cs ion current, and (2) Cs does not coat the electrical feedthroughs. The permanent gases in the gauge chamber are pumped externally with a pumping speed of approximately 1 liter/sec; typical gas pressure is 1×10^{-7} Torr.

The surface ionization detector itself consists of a 0.0075-cm-diam tungsten filament 3.8 cm long, carrying a current of 0.25 A and biased +100 V above the collector. The collector is a 2.5-cm-diam nickel cylinder 1.3 cm long and concentric with the filament. Ion current to the collector is measured with an electrometer. The ion current was found to be independent of filament bias and filament temperature (above the threshold).

The Cs gauge was calibrated against the known

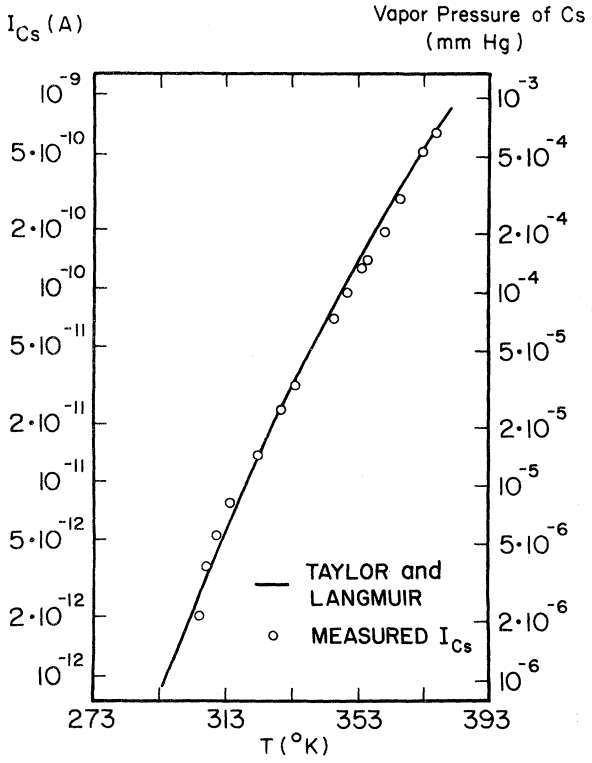

FIG. 3. Calibration of Cs gauge. Shown is measured Cs gauge current, I_{Cs}, versus the measured temperature of the Cs target chamber when the target chamber contained liquid Cs metal. Also shown, with a different ordinate, is the known vapor pressure of Cs versus temperature. The vapor pressure curve of Cs was calculated from the relationship given by Taylor and Langmuir, $\log_{10}p = 11.0531 - 1.35\log_{10}T - 4041T^{-1}$, where p is expressed in mm Hg and T is in °K. These measurements determine the calibration constant of the Cs gauge. (Marks indicating the values of the ordinates on the left and right scales are not intended to line up.)

vapor pressure[11] of Cs by having Cs vapor in equilibrium with liquid Cs in the oven. The temperature of the oven was measured with two thermocouples attached to the copper liner of the oven. Figure 3 shows a plot of the current in the Cs gauge, I_{Cs}, versus measured temperature of the target chamber when the chamber contained liquid Cs metal. Also shown, with a different ordinate, is the known vapor pressure of Cs versus temperature.[11] The ordinates of these two plots have been adjusted so that the Cs vapor pressure curve fits the measured I_{Cs} values as well as possible. Note that I_{Cs} is proportional to the Cs vapor pressure in the target chamber. Therefore, measurements similar to those of Fig. 3 are sufficient to determine the calibration constant of the Cs gauge. The Cs gauge can then be used to measure Cs vapor density in the target chamber.

After leaving the Cs oven, the beam passes through a magnetic field and enters the collection chamber where the separated charge component beams are measured. The positive and negative beams are each measured with a 2.5-cm-diam suppressed Faraday cup. The neutral atoms are measured with a detector which utilizes secondary electron emission. This neutral detector consists of a 2.5-cm-diam polished copper disc upon which the atoms are incident. The secondary electrons are collected on a 2.5-cm-diam ring located in front of the disc and concentric with it. The collection ring is biased at +180 V. To keep the secondary emitting surface clean, the polished copper disc is kept heated to 200°C, and the collection chamber is continually trapped with a large liquid-nitrogen-cooled trap.

In order to calibrate the neutral detector, it is necessary to determine the secondary electron current emitted from the copper surface per incident He^0 atom. The secondary emission ratio may be different for incident He^+. Because the fraction of He^- ions is small (less than 1%), the decrease in positive beam current as the Cs target density is increased is equal to the increase in the neutral beam. This statement is correct because the angular distribution of He^0 atoms formed by electron attachment in a gas target of low density is known to be such that almost all the fast atoms will exit from the target in a solid angle small enough to hit the neutral detector.[12] The plot of positive beam current as a function of secondary electron current (both divided by the source cup current) for various Cs target densities is a straight line whose slope is the secondary emission ratio. The secondary emission ratio was found to be constant to within 10% during the time required to measure a set of yield curves as a function of Cs target thickness at a particular energy, but changed as much as a factor of three for a particular energy over a period of weeks. The possibility that the secondary emission ratio depends on the state of excitation of the incident He^0 atom is discussed in Sec. V. The fractions of the beam emerging from the charge exchange cell in the positive, neutral and negative charge states are hereafter referred to as F_+, F_0, and F_-. By definition, $F_+ + F_0 + F_- = 1$. The total beam measured after passage through the target is generally greater than 95% of the beam measured before the target, except at very low energies or at very high Cs densities, where multiple scattering in the target causes loss of beam. A slight loss in beam occurs on passage of a beam through the target chamber with no Cs present because of a small misalignment of the apparatus.

The lifetime of the He^- ion has recently been reported[13] as 18.2 ± 2.7 μsec, which is much longer than the transit time in our apparatus, even at the lowest energies used (the transit time is 3.8 μsec at 1.5 keV).

III. DATA

Typical data are shown in Figs. 4–6 for incident He^+ energies of 3, 12, and 20 keV. The fractions F_+, F_0 and F_- of the beam with charge +1, 0, and −1 after passage of the beam through the Cs target are shown. The target thickness, π, is the product of density and path length, and is in units of atoms/cm^2.

Figure 7 shows the behavior of F_+ as a function of Cs target thickness for several energies, plot-

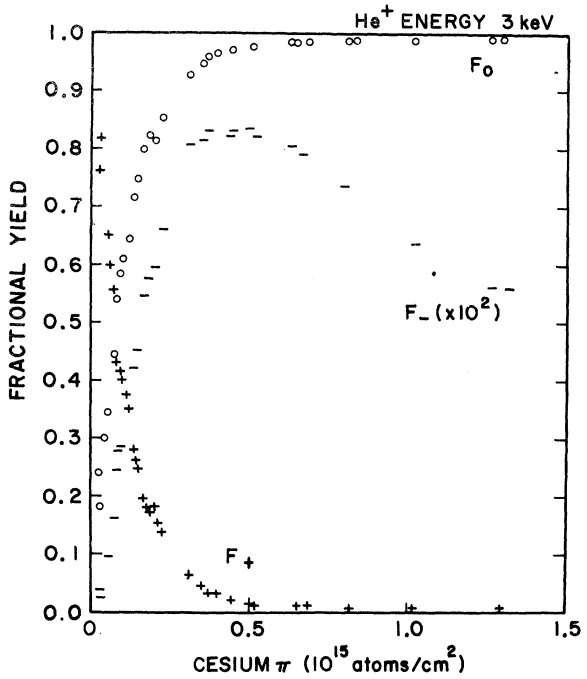

FIG. 4. The fraction of beam in the positive, neutral and negative charge states after passage of a 3-keV He^+ beam through a Cs vapor target, as a function of Cs target thickness, π. The negative fraction is multiplied by 100.

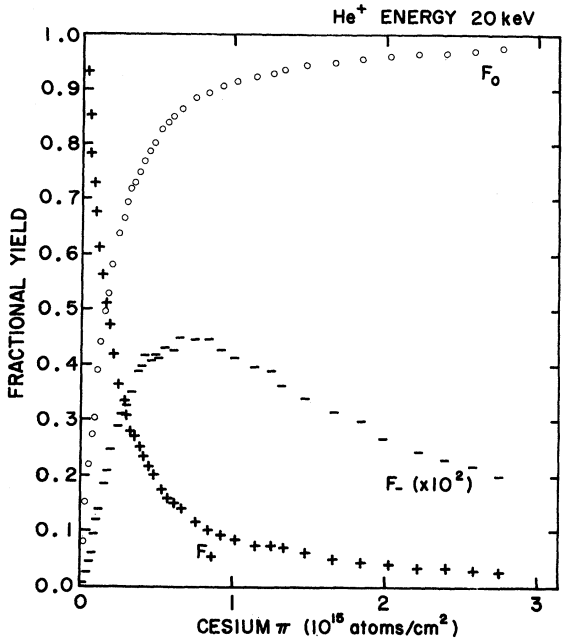

FIG. 6. The fraction of beam in the positive, neutral, and negative charge states after passage of a 20-keV He^+ beam through a Cs vapor target, as a function of Cs target thickness, π. The negative fraction is multiplied by 100.

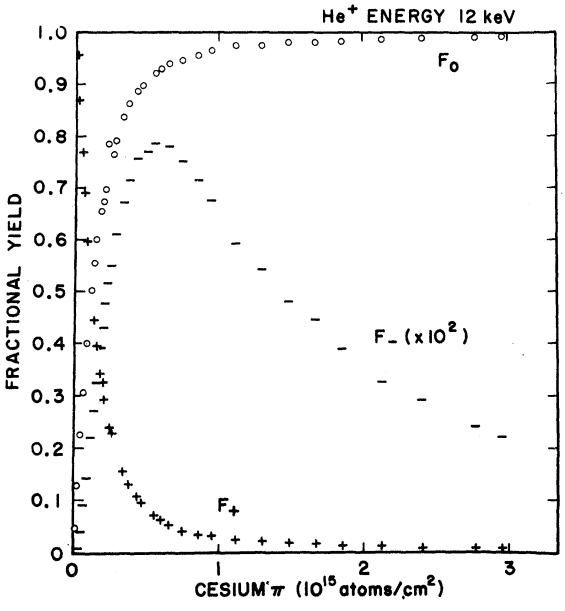

FIG. 5. The fraction of beam in the positive, neutral, and negative charge states after passage of a 12-keV He^+ beam through a Cs vapor target, as a function of Cs target thickness, π. The negative fraction is multiplied by 100.

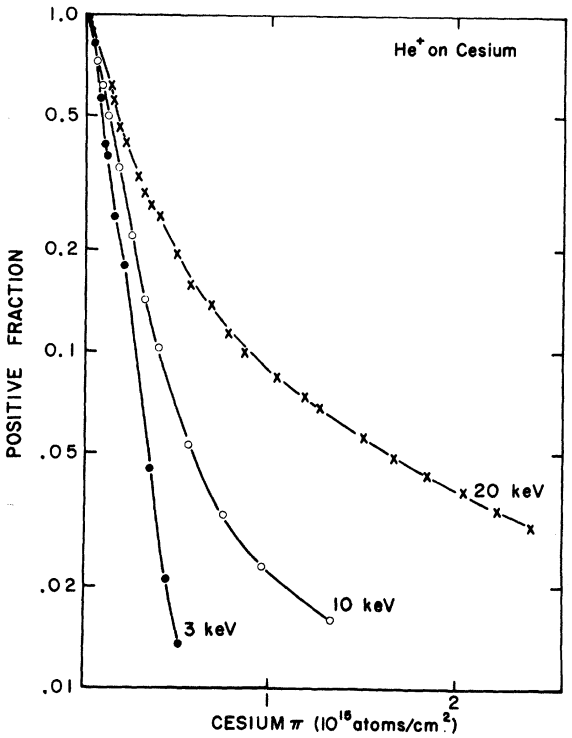

FIG. 7. The fraction, F_+, of beam in positive charge state as a function of Cs target thickness, π, after passage of a 3-, 10-, and 20-keV He^+ beam through a Cs vapor target. F_+ is shown on a logarithmic scale. The lines are drawn between points for clarity.

ted on a semilogarithmic scale. The lines between points are drawn for clarity. Note that for a He^+ energy of 3 keV, F_+ falls exponentially over two orders of magnitude as neutrals are created. This indicates that the positive ions are being neutralized but almost no neutrals are being stripped to form positive ions. At 20 keV, the positives are picking up electrons to form neutrals as well as being replenished by stripping of He^0 atoms, so that F_+ does not vary in a simple exponential fashion as a function of target thickness.

Figure 8 shows data for a very low Cs target thickness at a He^+ energy of 5 keV. Note that F_0 is linear at low densities, indicating a one-step process (single electron pickup).[14] F_- has virtually no linear region. Figure 9 shows F_- as a function of π^2: the linear portion indicates that the formation of He^- is primarily a two-step process.[14] Similar results were found by Donally,[3] who suggested that the primary mechanism in the formation of He^- is

$$He^+ + Cs \rightarrow He^0\ (1s)\ (2s)\ {}^3S_1 + Cs^+,$$
$$He^0\ (1s)\ (2s)\ {}^3S_1 + Cs \rightarrow He^-\ (1s)\ (2s)\ (2p)\ {}^4P_{5/2} + Cs^+$$

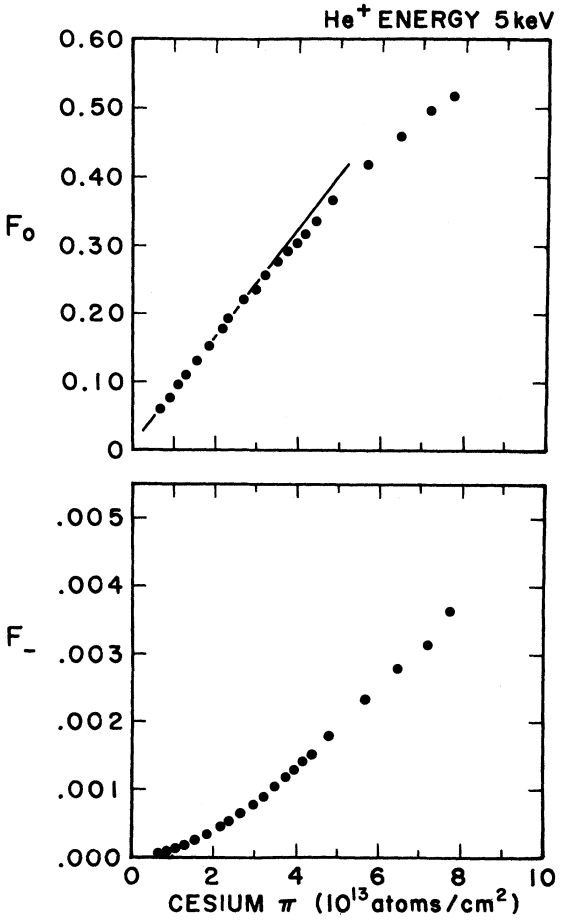

FIG. 8. The fractions, F_0 and F_-, of beam in neutral and negative charge states as a function of Cs target thickness, π, for a thin Cs target. The beam incident on the Cs target is He^+ at an energy of 5 keV. The line on the F_0 plot indicates the linear portion of the data (i.e., one-step process).

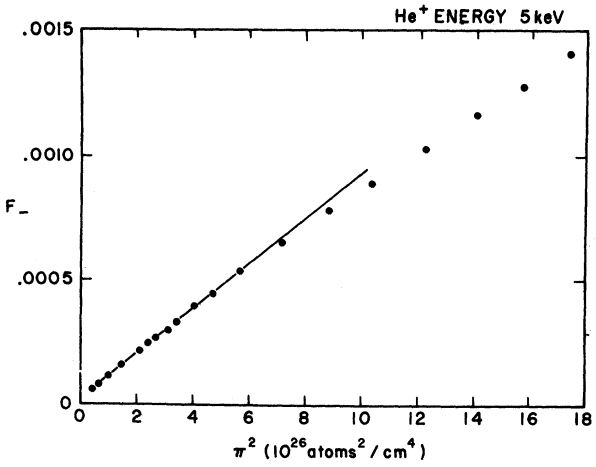

FIG. 9. The fraction, F_-, of beam in negative charge state as a function of the square of the target thickness, for 5-keV He^+ incident on a thin Cs target. The line indicates the region of the data in which the charge exchange is a two-step process.

IV. ANALYSIS

The experimental data consist of the three currents corresponding to He^+, He^0, and He^- beams as a function of Cs target thickness measured after passage of an initially positive beam through the Cs target. The cross section σ_{+0} can be obtained directly from the initial rate of loss of He^+ with Cs target thickness, since the initial growth of the He^- is very small. Further analysis is complicated by the existence of long-lived metastable singlet and triplet states. Only three charge components of the beam after passage through the target were measured experimentally. However, a model for the collisions must involve more than three components, because it was found impossible to fit the data with a three-component model using physically sensible cross sections.

Our apparatus does not measure the individual electronic state of the fast He ions or atoms leaving the target. Consequently, some discussion is necessary in order to know what electronic states of the He ions and atoms are important in our analysis of the data. The He^- ion has only one known electronic state, $(1s)\ (2s)\ (2p)\ {}^4P_{5/2}$.[1] The He^+ ions are probably in the ground state, $(1s)\ {}^2S_{1/2}$. The incident He^+ ions are entirely in the ground state, as any ions in excited states have been quenched. The He^+ ions which are produced in the Cs cell by stripping an electron from a fast He^0 are probably produced primarily in the $(1s)\ {}^2S_{1/2}$ state because of the difficulty of producing electronic excitations as large as 40.8 eV, the excitation energy to the $n = 2$ level, when the incident atoms have a kinetic energy in the range 1.5 to 25 keV.

In order to know the electronic state of the fast He^0 atoms, one must understand the collision processes in the target. A He^+ beam upon entering the Cs target is partially neutralized. The He^0 atoms may be produced in many possible states. Before the subsequent collision, the He^0 atoms will usually have time to decay into one of the following three states: $(1s)^2\ {}^1S_0$, $(1s)(2s)\ {}^1S_0$, or $(1s)(2s)\ {}^3S_1$. In analyzing our data, we have lumped both singlet states togeth-

er since we are able to obtain adequate fits to the data in this manner and since we are not able from our data to obtain information about reactions involving the individual long-lived singlet states. Obviously, this is an oversimplification of the actual situation. In our analysis, a cross section for production of a He^0 atom in a triplet state refers to production of the He^0 atom in either the $(1s)\,(2s)\,^3S_1$ state or in any state that decays to the metastable triplet state $(1s)\,(2s)\,^3S_1$ (i.e., production of a He^0 atom in any state of the triplet series). Reactions for production of some other state from a He^0 atom in a triplet state have the state $(1s)\,(2s)\,^3S_1$ as the initial state. Similar statements apply to the singlet cross sections (i.e., the cross section for production of a fast He^0 atom in a singlet state indicates the production of a He^0 atom in any state that decays to either the state $(1s)^2\,^1S_0$ or the state $(1s)\,(2s)\,^1S_0$).

The simplest model which fits the data is a set of four simultaneous first-order differential equations. The four components are positive and negative ions, and neutral atoms in triplet and singlet states (see the previous two paragraphs for the explanation of the states).

The four-component differential equations are

$$dF_+/d\pi = -(\sigma_{+t} + \sigma_{+s} + \sigma_{+-})F_+ + \sigma_{t+}F_t + \sigma_{s+}F_s + \sigma_{-+}F_-,$$

$$dF_t/d\pi = \sigma_{+t}F_+ - (\sigma_{t+} + \sigma_{ts} + \sigma_{t-})F_t + \sigma_{st}F_s + \sigma_{-t}F_-,$$

$$dF_s/d\pi = \sigma_{+s}F_+ + \sigma_{ts}F_t - (\sigma_{s+} + \sigma_{st} + \sigma_{s-})F_s + \sigma_{-s}F_-,$$

$$dF_-/d\pi = \sigma_{+-}F_+ + \sigma_{t-}F_t + \sigma_{s-}F_s - (\sigma_{-+} + \sigma_{-t} + \sigma_{-s})F_-.$$

Here, F_i refers to the fraction of the beam in the state i after passage through the target ($\Sigma_i F_i = 1$), and π is the Cs target thickness.

The differential equations were integrated simultaneously, using approximately 50 intervals of $\Delta\pi$. The initial values at $\pi = 0$ were the experimental conditions ($F_+ = 1$, $F_s = F_t = F_- = 0$). A nonlinear least-squares routine was used to adjust the cross sections in order to obtain the best fit to the experimental data. The fractions F_t and F_s were added for comparison with the experimental values of F_0. The criterion for judging that the fit of the model to the data was acceptable was $\chi^2 \lesssim 1$. In computing χ^2, the standard deviation, σ, at each datum point was taken to be 5% of the experimental value at that point.[15] This large an error was used in order to allow for systematic errors in the data.

An example of a fit of the charge-exchange model to the data is shown in Fig. 10 for a He^+ of energy 25 keV. The solid lines are the computed least squares fit; the dots are data points. The computed singlet and triplet fractions, F_S and F_t, and the computed ratio of F_t to F_0 (i.e., the fraction of He^0 atoms in the triplet state) are shown in Fig. 11. In his paper,[3] Donnally assumed that near $\pi = 0$, 75% of the neutrals were in the triplet state (which would be expected in the absence of spin-dependent processes in the electron pickup). In our fits to the data at various energies, we have found that near $\pi = 0$, $F_t/F_0 = 0.75 \pm 0.25$. This result is sufficient to show that Donnally's assumption is a fair approximation, but it is not sufficient to conclude an absence of spin-dependence in the electron pickup. It is also to be noted that the ratio F_t/F_0 decays exponentially with increasing π, as shown in Fig. 12 on a semilogarithmic plot for a He^+ energy of 25 keV.

After obtaining a fit to the data, uniqueness of the solution must be demonstrated, and confidence limits for the cross-section values must be determined. This was done by (1) computing χ^2 as each cross sections. An example of a contour in the constant, and (2) by computing contours of constant χ^2 in a space where the cross sections represent the coordinates. It was determined by the first method above that four cross sections (σ_{+-}, σ_{-+}, σ_{st}, σ_{s+}) could have values ranging from some upper bound to zero; for simplicity, these cross sections were then set equal to zero. Calculations at 25-keV He^+ energy showed that the remaining cross sections were essentially unaltered by this procedure.

Contours of constant χ^2 were computed, using a nonlinear estimation algorithm.[16] A contour with $\chi^2 \simeq 1$–2 was used to find confidence limits for the cross sections. An example of a contour in the

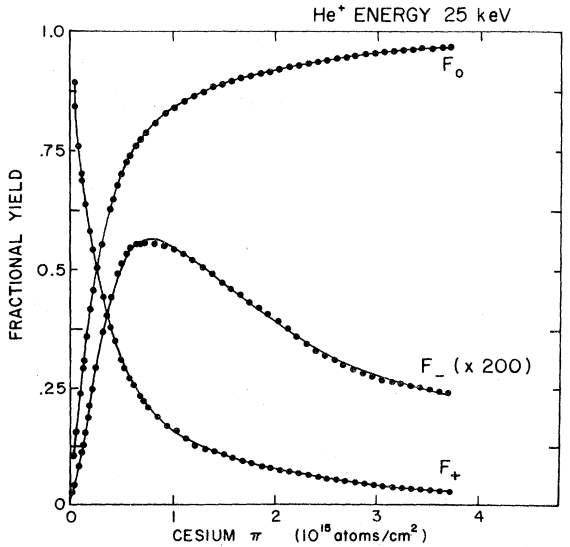

FIG. 10. Example of least-squares fit of charge-exchange model to data. The dots are experimental values of the fraction of beam in positive, neutral, and negative charge states after passage of a 25-keV He^+ beam through a Cs target. The solid lines are the computed fits of the model to the data. The fraction F_- is multiplied by 200.

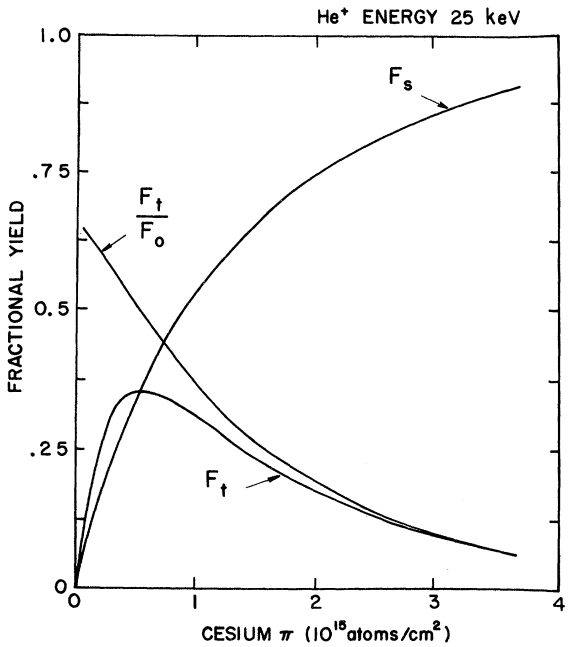

FIG. 11. Computed beam fractions from the model fit to the data shown in Fig. 10. Shown are the fractions of atoms in the singlet states and in the triplet state, and the ratio of the number of atoms in the triplet state to the number of all neutral atoms.

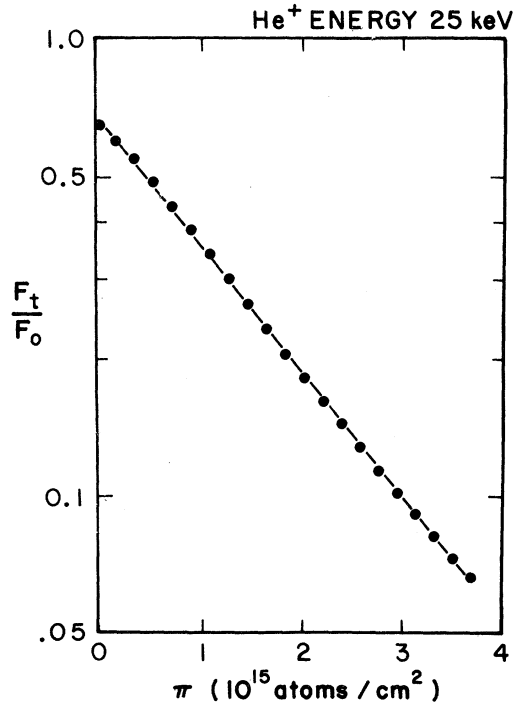

FIG. 12. The computed fraction of He^0 atoms in the triplet state, F_t/F_0, as a function of Cs target thickness. There is no direct experimental measurement of F_t/F_0. The dots are computed values of F_t/F_0 and the straight line is drawn through dots on a semilogarithmic plot merely to display the exponential decrease of F_t/F_0. This curve is the same as that shown in Fig. 11.

$\sigma_{+t} - \sigma_{+s}$ plane on which $\chi^2 \simeq 2$ is shown in Fig. 13 for a He^+ energy of 5 keV. The contour is nearly an ellipse. The major axis of the ellipse lies at an angle of 135° with respect to the σ_{+t} axis, and is therefore a locus of $\sigma_{+t} + \sigma_{+s}$ = constant. The projection of the ellipse on an axis gives the limits of confidence for that cross section, and the length of the minor axis gives the limits of confidence for the sum of the cross sections. The sum of the two cross sections is therefore determined with much greater precision than are the two individual cross sections. This arises because the total cross section, σ_{+0}, is determined explicitly from the experimentally measured initial rise of neutral atoms with increasing Cs target thickness, whereas the individual cross sections are not directly measured.

Cross sections were deduced from data with He^+ as the incident beam, rather than measured directly with a fast incident neutral beam, because the composition of the beam after neutralization in a permanent gas (i.e., the distribution between various long-lived singlet and triplet states) would be unknown. Further experiments are planned to examine the composition of a He^0 beam when He^+ ions undergo electron pickup in a gas target.

V. RESULTS AND DISCUSSION

The maximum yield of He^- ions after passage of a He^+ beam through Cs vapor is shown as a function of He^+ energy in Fig. 14. It is to be noted that the maximum value of F_- is not the equilibrium value. Each point has been assigned an error of ± 5%. The largest value of F_- is (1.4 ± 0.1)%, and this value occurs at a He^+ energy of 6 keV. Yields measured by Donnally and Thoeming[3] are also shown in Fig. 14; they give somewhat larger negative yields than our measurements. The Cs target thickness necessary for a maximum yield of He^- is $(5\pm1) \times 10^{14}$ atoms/cm² at energies below 10 keV, and rises to $(7 \pm 1) \times 10^{14}$ atoms/cm² at 25 keV. Our results for maximum yield of He^- are tabulated in Table I. All cross section results are tabulated in Table II.

The total charge-exchange cross section, σ_{+0}, is shown as a function of He^+ energy in Fig. 15. These data were taken from the initial slope of F_0 at low Cs target thicknesses (see Fig. 8), and are deter-

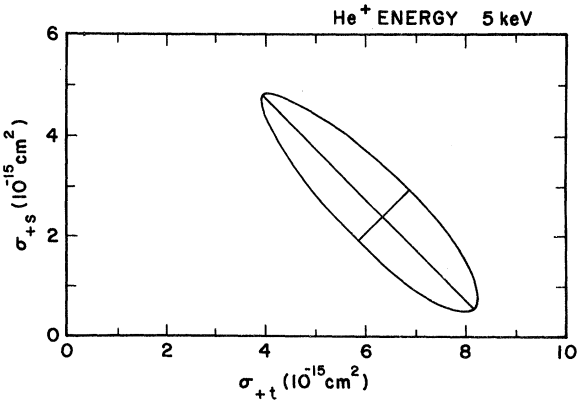

FIG. 13. Contour of $\chi^2 \simeq 2$ in the coordinate plane of σ_{+t} and σ_{+s}. The He^+ energy is 5 keV.

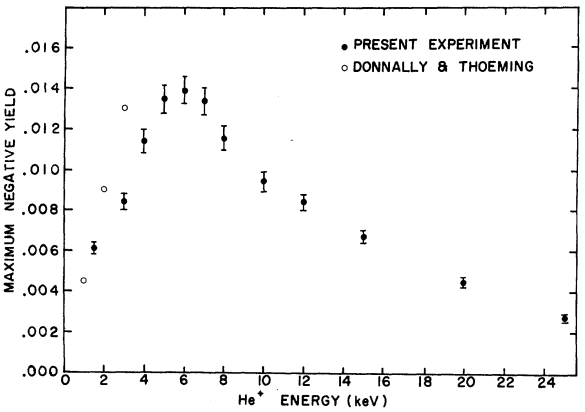

FIG. 14. Maximum yield of He^- ions after He^+ charge exchange in Cs, in the energy range 1.5–25 keV. Open circles are measurements by Donnally and Thoeming. The maximum yield is not an equilibrium yield.

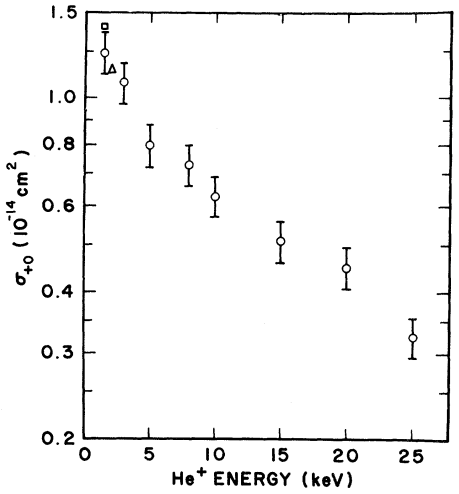

FIG. 15. The cross section σ_{+0} for He^+ on Cs, in the energy range 1.5–25 keV. The symbol □ is a measurement by Lorents and Peterson; the symbol △ is a measurement by Donnally and Thoeming.

TABLE I. Maximum yield of He^- after charge exchange of He^+ in Cs vapor, relative to total beam after passage through the target.

He^+ Energy (keV)	He^- yield (%)
1.5	0.61
3	0.84
4	1.14
5	1.35
6	1.39
7	1.34
8	1.16
10	0.94
12	0.84
15	0.67
20	0.45
25	0.27

TABLE II. Cross sections[a] for charge exchange of He^+ in Cs vapor, in units of 10^{-17} cm^2.

He^+ energy (keV)	σ_{+0}[b]	σ_{0-}	σ_{-0}	σ_{t+}	σ_{+t}[c]	σ_{+s}[c]	σ_{t-}	σ_{s-}	σ_{ts}	σ_{s+}	σ_{st}	σ_{+-}	σ_{-+}
1.5	1250 ± 120	20.5 ± 5.4	860 ± 270	5.4 ± 2.7	400	700	20 ± 5	< 2.8	27 ± 22	< 0.43	< 2.2	< 0.54	<49
3	1080 ± 110	19.5 ± 5.4	860 ± 270	12.0 ± 6.5	500	500	20 ± 5	3.4 ± 2.7	54 ± 43	< 1.7	< 5.4	< 0.32	<43
4		24.3 ± 5.4	970 ± 270	14.6 ± 8.1	650 ± 320	320 ± 320	24 ± 5	2.5 ± 1.9	60 ± 43				
5	800 ± 80	21.6 ± 5.4	810 ± 270	19 ± 11	650 ± 210	210 ± 210	20 ± 5	1.6 ± 1.1	70 ± 54	< 4.9	<11	< 0.38	<70
6		20.0 ± 5.4	760 ± 270	21 ± 11	650 ± 210	210 ± 210	20 ± 5	2.7 ± 1.9	76 ± 54				
7		19.5 ± 5.4	670 ± 220	27 ± 11	700 ± 160	160 ± 160	20 ± 5	< 1.9	150 ± 110	< 4.1	<11	< 0.32	<54
8	730 ± 70	17.3 ± 4.3	700 ± 220	29 ± 11	540 ± 160	160 ± 160	17 ± 5	1.3 ± 1.1	60 ± 43				
10	630 ± 60	14.0 ± 4.3	1030 ± 270	24 ± 11	700 ± 110	< 110	14 ± 4	< 1.0	65 ± 43	< 14	<27	< 0.38	<81
12		10.6 ± 2.7	730 ± 220	35 ± 16	500 ± 110	140 ± 110	10 ± 3	0.5 ± 0.4	76 ± 54				
15	510 ± 50	9.2 ± 2.2	760 ± 220	38 ± 16	480 ± 80	< 85	8.7 ± 2.1	1.0 ± 0.3	81 ± 54	< 3.8	<22	< 0.14	<70
20	450 ± 40	8.6 ± 2.2	1000 ± 270	60 ± 22	330 ± 54	87 ± 54	8.7 ± 2.1	0.7 ± 0.2	54 ± 43	< 1.9	< 5.4	< 0.08	<92
25	320 ± 30	5.7 ± 1.3	780 ± 160	108 ± 32	230 ± 50	92 ± 54	5.1 ± 1.3	0.5 ± 0.1	38 ± 32	< 1.2	< 2.2	< 0.16	<81

[a] Subscripts +, 0, s, t, and - refer to He atom or ion in charge state plus one, neutral (singlet and triplet), long-lived singlet, triplet metastable, and negative, respectively.

[b] The cross section σ_{+0} is not precisely the sum of σ_{+t} and σ_{+s}, because the listed values of σ_{+0} were determined from a more precise set of measurements.

[c] The cross sections σ_{+t} and σ_{+s} at 1.5 and 3 keV have uncertainties as large as the value.

mined to ±10%. Measurements of σ_{+0} by Lorents and Peterson[2] at 1.5 keV and by Donnally and Thoeming[3] at keV are also shown, and are in satisfactory agreement with ours. Combining our measurements of σ_{+0} with representative points from the measurements of Lorents and Peterson (Fig. 16) shows that σ_{+0} has a maximum value of approximately 1.3 $\times 10^{14}$ cm^2 at a He^+ energy of 1.5 keV. This large value of σ_{+0} presumably arises because the collision $He^+ + Cs^0 \rightarrow He^0\,(1s)\,(2s) + Cs^+$ is nearly resonant.

The cross section σ_{+0}, shown in Fig. 15, was determined from a series of measurements of the yield of neutral He atoms with very low Cs densities in the target chamber, as shown in Fig. 8. This cross section is of course also determined, but with less precision, from the analysis of the high-target-density yield curves as shown in Figs. 4–6. The values determined by the two methods are in agreement, as can be seen in Table II, by comparing σ_{+0} with the sum of σ_{+t} and σ_{+S}. The only reason for obtaining σ_{+0} from low-Cs-density yield curves rather than from the high-density yield curves is that the high-density yield curves do not have enough points at low densities to provide maximum precision. We would like to point out that our value of σ_{+0} at a He^+ energy of 1.5 keV is in agreement with the value measured by Lorents and Peterson in a different experiment; this provides evidence for the correctness of the calibration of our Cs gauge, since there are no adjustable parameters in our determination of σ_{+0}.

The cross sections σ_{-0}, σ_{t+}, and σ_{0-} are shown as functions of He^+ energy in Figs. 17–19. These cross sections were determined from the fit of the model to the data, and the error bars were determined from the $\chi^2 \simeq 1$ contours. Figures 20 and 21 show the cross sections σ_{+t}, σ_{+S}, σ_{t-}, and σ_{S-}. The precision of the determination of these cross sections is not as great as those previously discussed. The cross sections σ_{-t} and σ_{-S} could not be determined individually at all; only the sum σ_{-0} was determined.

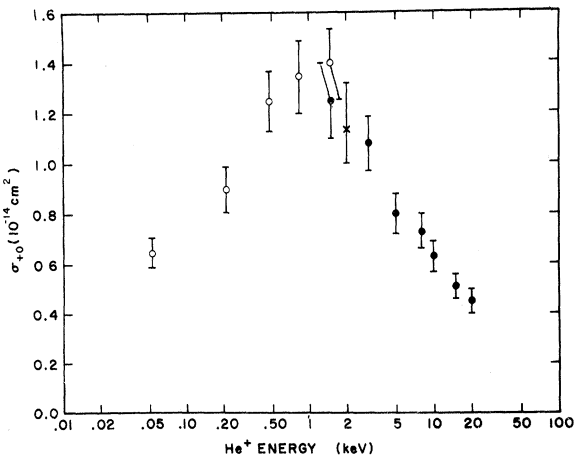

FIG. 16. The cross section σ_{+0} for He^+ on Cs, in the energy range 0.05–20 keV, showing measurements by Lorents and Peterson (open circles), our measurements (closed circles), and measurement by Donnally and Thoeming (symbol ×).

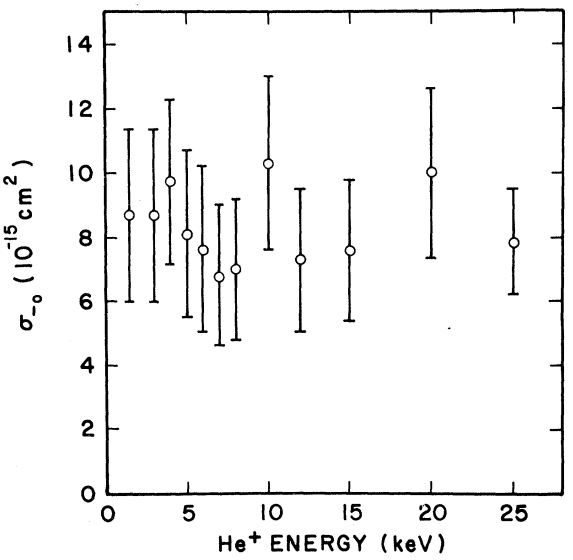

FIG. 17. The cross section σ_{-0} for He^+ on Cs.

The cross section σ_{t-} is about an order of magnitude greater than the cross section σ_{S-}, which confirms Donnally's suggestion[3] that the He^- ion is formed primarily by electron pickup from the metastable triplet state. The reason for this, as he pointed out in his paper, is that He^- is believed to be in a quartet state. Therefore, the production of He^- by the charge-changing collision of a He^0 atom in a singlet state and a Cs atom would require a simultaneous spin flip and pickup of a $2p$ electron. The collision time is too short for this to be a significant process.

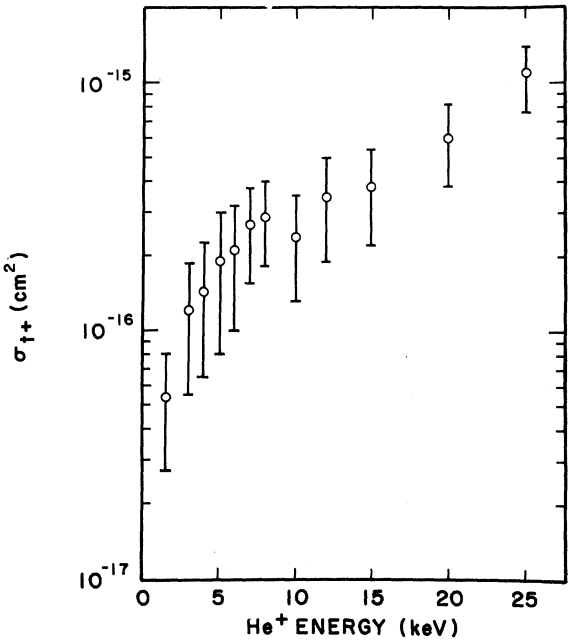

FIG. 18. The cross section σ_{t+} for He^+ on Cs.

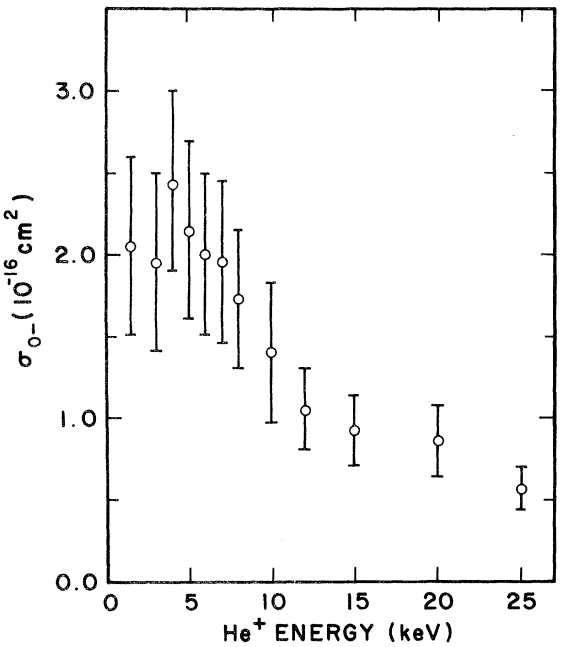

FIG. 19. The cross section σ_{0-} for He^+ on Cs.

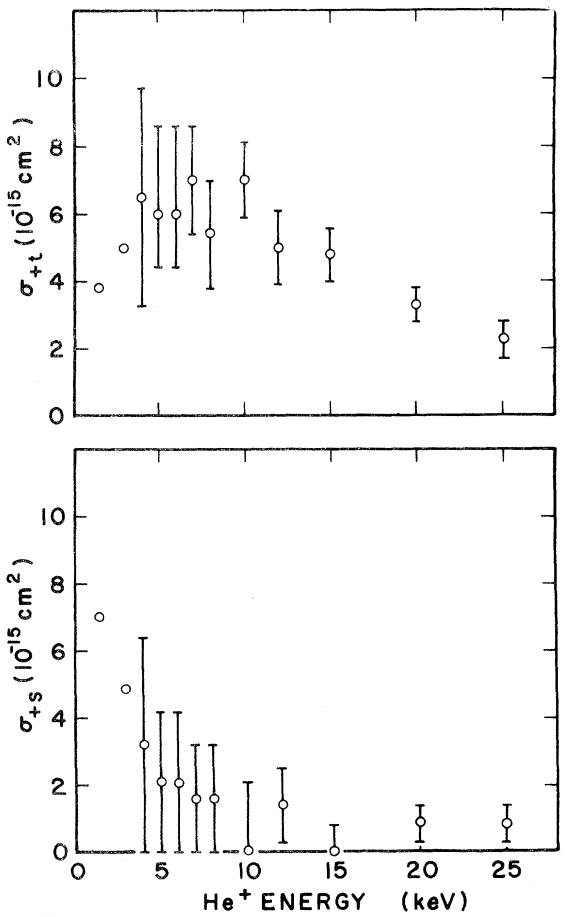

FIG. 20. The cross sections σ_{+t} and σ_{+s} for He^+ on Cs. Points at 1.5 and 3 keV have uncertainties as large as the value.

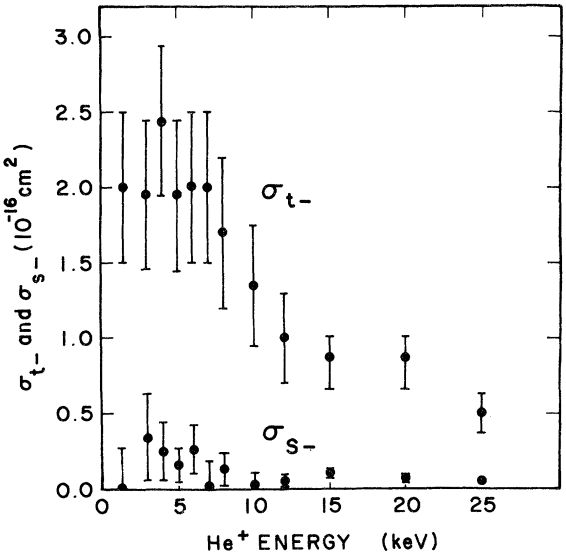

FIG. 21. The cross sections σ_{t-} and σ_{s-} for He^+ on Cs. Note that the cross section σ_{t-} is approximately an order of magnitude larger than the cross section σ_{s-}.

The cross sections σ_{+l} and σ_{+s} were not determined with sufficient precision to be able to find whether σ_{+l} is three times as large as σ_{+s}. This would be expected if the excited helium atoms after collision were statistically distributed between singlet and triplet states, as would be the case in the absence of spin-dependent processes in the electron pickup.

The cross section σ_{-0} is independent of He^+ energy over the energy range measured, and has a value of $(9 \pm 3) \times 10^{-15}$ cm^2. The cross section σ_{0-} has a value of $(2.4 \pm 0.5) \times 10^{-16}$ cm^2 at an approximate He^+ energy of 4 keV.

Approximate upper bounds were determined for σ_{+-}, σ_{-+}, σ_{s+}, and σ_{st}. They are shown in Table II. These upper bounds were determined by individually introducing each cross section into the model, and then determining its value such that $\chi^2 \simeq 1$.

The cross section σ_{t+} is about an order of magnitude larger than σ_{s+}. This might be expected if the singlet atoms are mostly in the ground state, because of the large energy required for ionization relative to the energy necessary for ionization from the $(1s)$ $(2s)$ triplet state.

The cross sections σ_{ts} and σ_{st} could not be reliably determined. The cross section σ_{ts} is of the order of $(7 \pm 5) \times 10^{-16}$ cm^2, while σ_{st} has an upper bound about one order of magnitude less. Only an upper bound on the two-electron exchange cross sections, σ_{+-} and σ_{-+}, could be determined. The upper bounds are 5×10^{-18} cm^2 for σ_{+-}, and 9×10^{-16} cm^2 for σ_{-+}.

We are in agreement with Donnally, to within the stated accuracy, for σ_{t-}, σ_{-0}, and $(\sigma_{ts} + \sigma_{t-})$.

There are a number of systematic errors associated with this experiment. (1) Data taken with the Cs density increasing differs systematically from that taken with the Cs density decreasing. This effect has been included in the data by allowing ± 5% error at each datum point. (2) The calibration constant

of the Cs gauge slowly changed with time (50% drift over the entire course of these measurements). One possible explanation for the changing calibration constant of the gauge is that the probability of a Cs atom sticking to the cold surface in the gauge might slowly change as the surface becomes less clean. The Cs gauge calibration was therefore checked periodically, and drift contributes at most ± 10% error to the cross sections. In addition to this 10% error, the absolute calibration of the Cs gauge to the Cs vapor pressure has an uncertainty of ±20%. (3) We have some evidence that the yield of secondary electrons from the copper secondary emitting surface is different when incident He atoms are in triplet or singlet states. That this is true at thermal energies is well known.[17] Further study of this is planned. If the secondary emission is found to be significantly different for singlet and triplet He^0 atoms, then the values of the cross sections could be affected. The maximum yield of He^- ions would not be significantly affected, because the transmission through the target is 95%; the value of σ_{+0} would not be affected, because the triplet fraction in the beam does not change appreciably at the low Cs densities used for the determination of this cross section.

We would like to clearly point out that only the relative errors associated with the various cross sections are quoted throughout this paper. The 20% uncertainty in the calibration of the Cs gauge must be added to the quoted error in order to obtain the precision of the absolute cross sections.

We would also like to point out that during this experiment the following experimental procedures were observed. (1) Transmission of the beam was monitored by measurement immediately before the target and by measurements of all three beam components after passage through the target; (2) care was taken to subtract effects due to collisions with background gases; and (3) the secondary emission ratio of the neutral beam detector was monitored during each set of measurements.

ACKNOWLEDGMENT

We would like to acknowledge the able assistance of Steven Vigdor during this experiment.

---

*This research was supported by U. S. Army Research, Durham, North Carolina; The U. S. Atomic Energy Commission; and The University of Wisconsin Research Committee with funds provided by a NASA institutional grant and with funds for computer use.

[1]E. Holøien and J. Midtdal, Proc. Phys. Soc. (London) 68, 815 (1955). See also E. Holøien and J. Midtdal, Proc. Phys. Soc. (London) 90, 883 (1967).

[2]D. C. Lorents and J. B. Peterson, Abstracts of Papers of the Fourth International Conference on Physics of Electronic and Atomic Collisions (Science Bookcrafters, Hastings-on Hudson, N. Y., 1965), p. 328. See also H. G. Dehmelt and F. G. Major, Phys. Rev. Letters 8, 213 (1962).

[3]B. L. Donnally and G. Thoeming, Phys. Rev. 159, 87 (1967).

[4]T. Jorgensen, Jr., C. E. Kuyatt, W. W. Lang, D. C. Lorents, and C. A. Sautter, Phys. Rev. 140, A1481 (1965).

[5]R. M. Ennis, Jr., D. E. Schechter, G. Thoeming, D. B. Schlafke, and B. Donnally, IEEE Trans. Nucl. Sci. 14, 75 (1967).

[6]P. Mahadevan, C. E. Carlston, and G. D. Magnuson, Bull. Am. Phys. Soc. 10, 692 (1965).

[7]F. A. Rose, P. B. Tollefsrud, and H. T. Richards, IEEE Trans. Nucl. Sci. 14, 78 (1967).

[8]J. P. Aldridge, J. John, C. P. Robinson, W. J. Wallace, K. R. Chapman, and R. H. Davis, Bull. Am. Phys. Soc. 12, 462 (1967).

[9]J. John, C. P. Robinson, J. P. Aldridge, W. J. Wallace, K. R. Chapman, and R. H. Davis, IEEE Trans. Nucl. Sci. 14, 82 (1967).

[10]N. F. Ramsey, Molecular Beams (Oxford University Press, London, 1956), p. 379.

[11]J. Taylor and I. Langmuir, Phys. Rev. 51, 753 (1937); and L. L. Marino, A. C. H. Smith, and E. Caplinger, *ibid.* 128, 2243 (1962).

[12]P. R. Jones, F. P. Ziemba, H. A. Moses, and E. Everhart, Phys. Rev. 113, 182 (1959); A. B. Wittkower and H. B. Gilbody, Proc. Phys. Soc. (London) 90, 343 (1967). A. B. Wittkower, P. H. Rose, R. P. Bastide, and N. B. Brooks, Phys. Rev. 136, A1254 (1964).

[13]D. J. Nicholas, C. W. Trowbridge, and W. D. Allen, Phys. Rev. 167, 38 (1968).

[14]S. K. Allison, Rev. Mod. Phys. 30, 1137 (1958). The solution for a beam fraction can be expanded in powers of π, each successive term in the expansion indicating a higher-order collision.

[15]The data were analyzed in the following manner. A smooth curve was drawn through the experimental data points for the F's. About 50 points at approximately equal spacings were read off the curve for each of the three F's, and these 150 points were treated as the experimental data points. Although the number of points taken, 50 for each F, was chosen for convenience, the number of experimental data points was approximately this large. The best fit to the data was found by varying the cross sections to minimize the quantity.

$$\chi^2=\frac{1}{150}\sum\frac{(F_{\text{exp}}-F_{\text{calc}})^2}{(0.05F_{\text{exp}})^2}.$$

The standard deviation of each measurement was arbitrarily taken as $0.05F_{\text{exp}}$ in order to allow for systematic errors.

[16]G. W. Booth and T. I. Peterson, American Institute of Chemical Engineering Computer Program Manual No. 3, 1960 (unpublished). We would like to express our appreciation to Mr. Peter J. Wolfe of the University of Wisconsin Computing Center for his assistance in adapting this method to our problem.

[17]M. Kaminsky, Atomic and Ionic Impact Phenomena on Metal Surfaces (Academic Press Inc., New York, 1965), p. 300.